



STRUCTURAL DAMAGE DIAGNOSIS METHOD BASED ON SUBSPACE IDENTIFICATION METRIC

Helói Francisco Gentil Genari

Eurípedes Guilherme de Oliveira Nóbrega

Department of Computational Mechanics, Mechanical Engineering Faculty, State University of Campinas, Campinas, Brazil
 e-mails: hegenari@fem.unicamp.br, egon@fem.unicamp.br

Nazih Mechbal

Laboratory of Process and Engineering in Mechanics and Materials, Arts et Métiers ParisTech, Paris, France
 e-mail: nazih.mechbal@ensam.eu

Abstract. *In this paper, experimental results related to structural damage diagnosis are presented, including damage detection, severity analysis and localization. The original approach used in this study is based on the assessment of a distance metric between infinite observability matrices experimentally identified using data from healthy and damaged structures, through an output-only subspace-based identification algorithm. Time series analysis of vibration signals from an aluminum plate, measured with and without damaged conditions, conducts to identification of ARMA models in a state-space form. A reference model for the undamaged plate is selected and current measurements of damaged plate are compared to this signature using the adopted subspace metric. Analysis of results indicates that the method can be applied for efficient severity analysis, localization and detection of damages in real structures.*

Keywords: *damage detection, severity analysis and localization, subspace metric, subspace identification and experimentation*

1. INTRODUCTION

Mechanical structures are subjected to aging from repetitive strain, friction, loads, and differences in temperatures and pressures. Furthermore, parts of these structures can be in contact with rain, moisture and other corrosive agents. Thus, the combination of these physical and chemical agents contributes significantly to structure deterioration. An efficient detection of damage can prevent catastrophic failures and save maintenance costs. Thereby, in these last decades, damage detection techniques and structural health monitoring (SHM) have been investigated, and several damage indicators have been proposed in literature (Fan and Qiao, 2010; Genari and Nobrega, 2012; Fassois and Sakellariou, 2007).

Structural vibration characteristics, such as frequency, vibration modes and damping, are directly influenced by physical properties, such as mass and stiffness. Damage reduces the stiffness and/or the mass of the structure, and so alters the dynamical response (Humar *et al.*, 2006). Damage detection methods based on vibration characteristics use changes in modal frequencies, mode shapes and flexibility matrix as a damage indicator (Carden and Fanning, 2004; Worden and Dulieu-Barton, 2004; Saeed *et al.*, 2009a,b).

Time-series analysis-based methods, a subclass of vibration-based methods, are another important category for damage detection. For example, Lu and Gao (2005) considered the standard deviation of residual error of auto-regressive with exogenous input (ARX) models for fault detection; Nair *et al.* (2006) considered only the first three AR coefficients of the auto-regressive moving-average (ARMA) model to define a damage-sensitive feature. Zhen and Zhigao (2010) proposed a technique to detect damage of offshore platform structures based on the fact that auto-regressive coefficients are function of the structure's eigenvalues. Fassois and Sakellariou (2007) made a general revision of the time-series methods for fault detection. One important feature of fault detection and structural health monitoring using time-series is that it is not necessary to know the underlying model under healthy stats. Furthermore, they may be conveniently applied when only the resultant vibration is possible to measure, and the correspondent excitation is unknown or not accessible.

Considerable part of time-series damage detection methods uses the system identification techniques to obtain modal properties from measured signals. The stochastic subspace identification has received great attention from the scientific community to be efficient in extracting the desired damage features and damage detection (Ren *et al.*, 2011). For instance, Bodeux and Golinval (2003) presented results of modal identification and damage detection on the Steel-Quake structure using the autoregressive moving average vector and data-driven stochastic subspace methods. Inocente-Junior *et al.* (2009) used subspace identification and residue generation for SHM in real beams. Genari and Nobrega (2012) showed that cepstral metric technique together with stochastic subspace identification can be used for damage detection in real structures.

ARMA models are commonly assumed when time-series analysis is involved. A cepstral metric for distance evaluation between models was originally introduced by Martin (2000), and subsequently a subspace metric was proposed by De Cock and De Moor (2002), expressed as angles between identified models. Zheng and Mita (2008) adopted both metrics

as damage indicators, and applied it to a mathematical model of a structure with five storeys, subjected to simulated ambient and earthquake excitations and stiffness reduction as damage. Experimental results of monitoring a building using cepstral-based SHM method were presented by Zheng and Mita (2007) considering a low frequency range and five vibration modes. Despite the good prospect of these methods as damage indicators, experimental results for the subspace method are not published yet. Also, several aspects of the application of the method to structures regarding severity and a more precise damage localization are not yet adequately studied.

In this paper, a subspace metric for damage detection and diagnosis, considering a medium frequency range analysis, is experimentally studied, using an aluminum plate with piezoelectric sensors and actuators, and different simulated damages. Initially, several measured time series of the plate with and without damage are used to identify state-space models based on an output-only subspace method. Thereafter, the undamaged and damaged plate models are compared through the adopted subspace metric. Differences between models are used as a damage indicator, and an analysis of severity and localization is conducted. Results show that using medium frequency range is a promising way to detect damage and to assess its severity.

2. BASIC THEORY

The damage detection methodology is represented by the flowchart of Fig. 1. The first step is the signal acquisition of input and output of the structure. By using subspace identification, based on output-only method, the ARMA models are obtained. Reference ARMA models are identified from normal structure vibration signals, while the new ARMA models are obtained from damaged structure vibration signals. Then, damage indicators are computed as the distance between models using subspace metric. The following subsections describe each block of the flowchart.

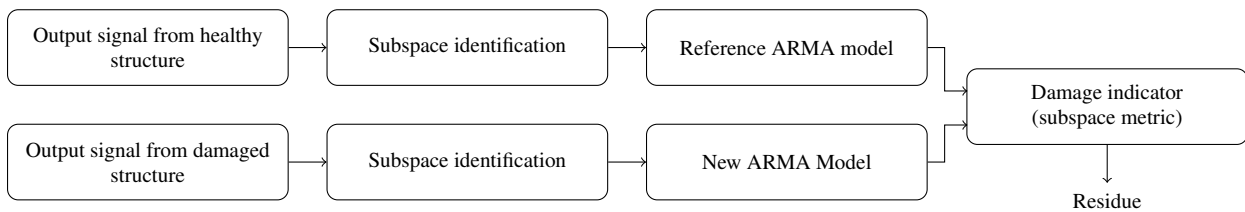


Figure 1. Flowchart of damage detection methodology

2.1 Subspace metric

An ARMA model, linear, time-invariant, stable and minimum phase, can be described by the forward innovation state-space form:

$$\begin{aligned} x(k+1) &= Ax(k) + Ke(k) \\ y(k) &= Cx(k) + e(k) \end{aligned} \quad (1)$$

in which $e(k)$ is the innovation process, K is the Kalman gain, $x(k)$ is the state vector, $y(k)$ is the output of the model and A and C are deterministic matrices.

Assuming that $H(z)$ is the transfer function in z -domain of the model expressed by Eq. (1), cepstrum coefficients of $H(z)$ are defined as:

$$\sum_{m \in \mathbb{Z}} c(m)z^{-m} = \log(H(z)\bar{H}(z^{-1}))$$

in which \bar{H} denotes the complex conjugate of $H \in \mathbb{C}$.

Martin (2000) defines the distance between two ARMA models M_1 and M_2 with transfer functions $H_1(z)$ and $H_2(z)$ as the distance between its cepstrum coefficients, given by:

$$D_M(M_1, M_2)^2 = \sum_{m=1}^{\infty} m |c_1(m) - c_2(m)|^2$$

De Cock and De Moor (2002) expressed the cepstral metric directly in terms of the principal angles between infinity observability spaces. For instance, let $M_1 = (A_1, K_1, C_1)$ and $M_2 = (A_2, K_2, C_2)$ be two ARMA models with infinite observability matrix defined by:

$$\mathcal{O}_{\infty}(M_i) = \begin{bmatrix} C_i & C_i A_i & C_i A_i^2 & \ddots \end{bmatrix}^T$$

Then, the distance between M_1 and M_2 can be calculated in terms of the principal angles between the subspace ranges $[\mathcal{O}_\infty(M_1) \quad \mathcal{O}_\infty(M_2^{-1})]$ and $[\mathcal{O}_\infty(M_2) \quad \mathcal{O}_\infty(M_1^{-1})]$, where $M_i^{-1} = (A_i - K_i C_i, K_i, -C_i)$ is the inverse model of M_i . Thus, the distance defined by Martin (2000) can be written equivalently as:

$$D_s(M_1, M_2)^2 = \log \prod_{i=1}^{2n} \frac{1}{\cos^2 \theta_i}$$

in which θ_i is i^{th} principal angle between these spaces and n is the model order.

It can be proved that it is sufficient to consider AR parameters to measure distance between two ARMA models (Martin, 2000; Zheng and Mita, 2007). Thus, let $M_1 = (A_1, C_1)$ and $M_2 = (A_2, C_2)$ represent two AR models with order n . Then, the subspace metric is equal to:

$$D_s(M_1, M_2)^2 = \log \prod_{i=1}^n \frac{1}{\cos^2 \theta_i} \quad (2)$$

where θ_i are the principal angles between the subspace ranges $\mathcal{O}_\infty(M_1)$ and $\mathcal{O}_\infty(M_2)$. Notice that $\mathcal{O}_\infty(M_i) = -\mathcal{O}_\infty(M_i^{-1})$ when K of Eq. (1) is null and this implies that it is necessary to calculate only n subspace angles between the infinite observability matrices of M_1 and M_2 .

2.2 Subspace identification

Consider a stochastic linear time-invariant system in a state-space discrete-time representation:

$$\begin{aligned} x(k+1) &= Ax(k) + \omega(k) \\ y(k) &= Cx(k) + e(k), \quad k = k_0, k_0 + 1, \dots \end{aligned} \quad (3)$$

in which k_0 is the initial time index, $x \in \mathbb{R}^{n \times 1}$ is the state vector, $y(k) \in \mathbb{R}^{p \times 1}$ is the observation vector, and $A \in \mathbb{R}^{n \times n}$ and $C \in \mathbb{R}^{p \times n}$ are deterministic matrices. The vector $\omega \in \mathbb{R}^{n \times 1}$ is the plant noise and $e \in \mathbb{R}^{p \times 1}$ is the observation noise vector. Both of these noise vectors have with zero mean and have as covariance matrices Q , R and S such as:

$$E \left\{ \begin{bmatrix} \omega(k) \\ e(k) \end{bmatrix} \begin{bmatrix} \omega^T(s) & e^T(s) \end{bmatrix} \right\} = \begin{cases} \begin{bmatrix} Q & S \\ S^T & R \end{bmatrix}, & \text{if } k = s \\ 0, & \text{if } k \neq s \end{cases}$$

where $E\{\cdot\}$ represents mathematical expectation, $R \in \mathbb{R}^{p \times p}$ is positive definite and $Q \in \mathbb{R}^{n \times n}$ is nonnegative definite.

The model described by Eq. (3) can be converted into a forward innovation model through the application of the Kalman filter (Desai and Pal, 1982). Considering $\omega(k) = Ke(k)$ and $e(k) = y(k) - Cx(k)$, the forward innovation model represented by Eq. (1) is obtained.

Thus, for system identification of the ARMA model in the forward innovation state-space form, it is necessary to estimate matrices A and C , and Kalman gain K . However, for the application in this paper, only the AR part of the ARMA model is considered. Therefore, only the estimation of matrices A and C is needed. Methods that include estimation of K are described in (Overschee and Moor, 1996; Katayama, 2005).

In most damage detection applications, the excitation is unknown and it is necessary to use output-only methods for system identification. In this paper, only the output data is used to estimate matrices A and C .

The Hankel form is depicted as the covariance matrix between past and future output data of the time series, i.e:

$$\begin{aligned} H_{k,k} &= E \left[\begin{pmatrix} y(k+1) \\ y(k+2) \\ y(k+3) \\ \vdots \\ y(k+k) \end{pmatrix} \begin{pmatrix} y(k)^T \\ y(k-1)^T \\ y(k-2)^T \\ \dots \\ y(k-k+1)^T \end{pmatrix}^T \right] \\ &= \begin{bmatrix} \Lambda(1) & \Lambda(2) & \dots & \Lambda(k) \\ \Lambda(2) & \Lambda(3) & \dots & \Lambda(k+1) \\ \vdots & \vdots & \ddots & \vdots \\ \Lambda(k) & \Lambda(k+1) & \dots & \Lambda(2k-1) \end{bmatrix} \end{aligned}$$

where $\{\Lambda(l) = E\{y(k+l)y(k)^T\}, l = 0, 1, \dots, L\}$, $2k-1 \leq L$ and $p(k-1) \geq n$.

The Hankel matrix can be decomposed, if $\text{rank}(H_{k,k}) = n$, as:

$$H_{k,k} = O_k \Gamma_k \quad (4)$$

in which O_k and Γ_k are extended observability and reachability matrices, respectively, defined as:

$$O_k = \begin{bmatrix} C \\ CA \\ \vdots \\ CA^{k-1} \end{bmatrix}, \quad \Gamma_k = [\bar{C}^T \quad A\bar{C}^T \quad \dots \quad A^{k-1}\bar{C}^T]$$

where $\bar{C} = E\{y(k)x^T(k+1)\}$.

The singular value decomposition of $H_{k,k}$ is given by:

$$H_{k,k} = [U_n \quad U_r] \begin{bmatrix} \Sigma_n & 0 \\ 0 & \Sigma_r \end{bmatrix} \begin{bmatrix} V_n^T \\ V_r^T \end{bmatrix} = U_n \Sigma_n V_n^T \quad (5)$$

in which Σ_n contains the largest n singular values of $H_{k,k}$.

Comparing Eq. (4) with Eq. (5), the extended observability and reachability matrices become

$$O_k = U_n \Sigma_n^{\frac{1}{2}}, \quad \Gamma_k = \Sigma_n^{\frac{1}{2}} V_n^T$$

The upward shift of the extended observability matrix generates the following identity

$$\begin{bmatrix} C \\ CA \\ \vdots \\ CA^{k-2} \end{bmatrix} A = \begin{bmatrix} CA \\ CA^2 \\ \vdots \\ CA^{k-1} \end{bmatrix} \iff O_{k-1} A = O_k(p+1; kp, 1:n)$$

where A is obtained through the least squares solution.

The matrices C and \bar{C}^T are computed from the extended observability and reachability matrices, respectively, as

$$C = O_k(1:p, 1:n), \quad \bar{C}^T = \Gamma_k(1:n, 1:p)$$

2.3 Damage indicator

In this work, the distance measure between AR models is considered to be a damage indicator. Assuming that a reference model is obtained of the healthy structure and there exists a model representing the damaged structure, the difference between the two models is correlated with the position and severity of the damage. To quantify the distance between AR models, a subspace metric for AR models is adopted. From Eq. (2), the following damaged indicator is proposed:

$$D_s(M_1, M_2) = \sqrt{\log \prod_{i=1}^n \frac{1}{\cos^2 \theta_i}}$$

where the matrices $\mathcal{O}_\infty(M_1)$ and $\mathcal{O}_\infty(M_2)$ used to calculate the principal angles θ_i are obtained by on-line identification using the previous approach.

3. EXPERIMENTAL RESULTS

3.1 Setup description

The experimental setup consists of a rectangular aluminum plate supported by foam to simulate free vibration. The plate has sides measuring 700mm per 500mm and thickness measuring 1mm (Fig. 2).

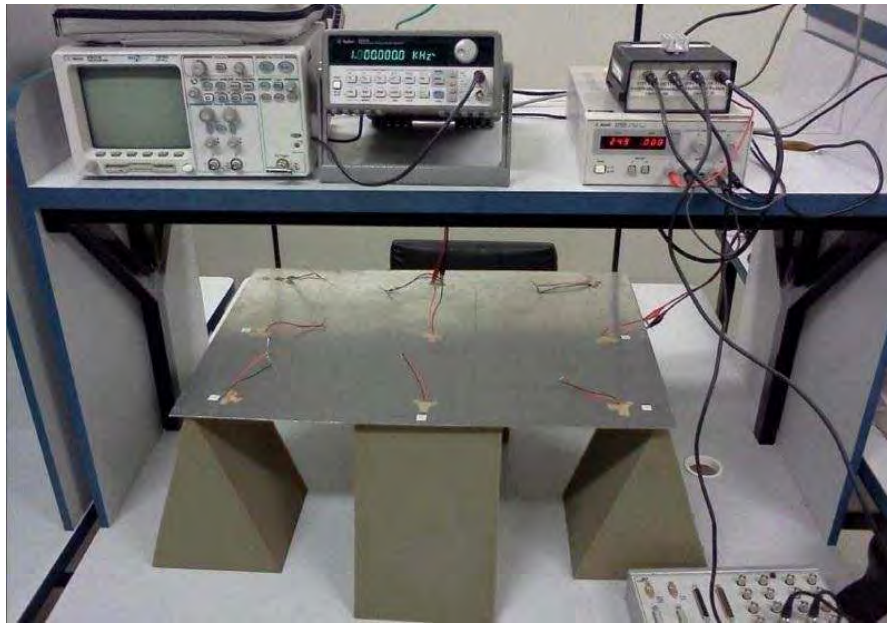


Figure 2. Experiment setup

The plate is mounted with nine piezoelectric elements, eight piezoelectric elements as sensors (s_1, s_2, \dots, s_7 and s_8) and one piezoelectric element as actuator (a_1), as shown in Fig. 3. The precise location of the sensors and the actuator, using the reference axis of Fig. 3, is presented in Tab. 1.

Table 1. Location of the sensors and the actuator.

axis	a_1	s_1	s_2	s_3	s_4	s_5	s_6	s_7	s_8
x (mm)	0	-280	-280	-280	0	280	280	280	0
y (mm)	0	-200	0	200	200	200	0	-200	-200

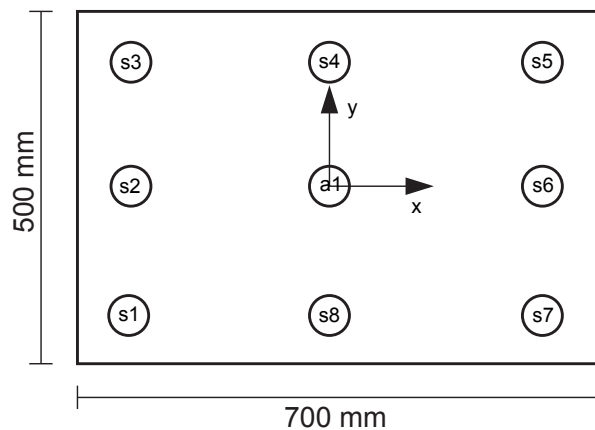


Figure 3. Sensors and actuator positions

For each pair of sensor and actuator ($a_1 - s_i$), a single-input and single-output (SISO) transfer function is considered. For instance, $a_1 - s_1, \dots, a_1 - s_8$ are all the possible SISO systems and are named in the sequel: s_1, \dots, s_8 , respectively.

3.2 Damage monitoring

A dSPACE® board, model DS 1104 and ControlDesk® software are used for the signal generation and data acquisition. The excitation signal is amplified and applied to a piezoelectric transducer. The vibration signal is captured by the other piezoelectric sensors, amplified and transmitted to acquisition. The block diagram of experimental setup is presented in Fig. (4). In this experiment, white noise signal with average zero and variance 0.4, sampled at 20kHz and with 50000 points, was applied as excitation signal and its response is here analysed in the frequency range from 2kHz to 10kHz.

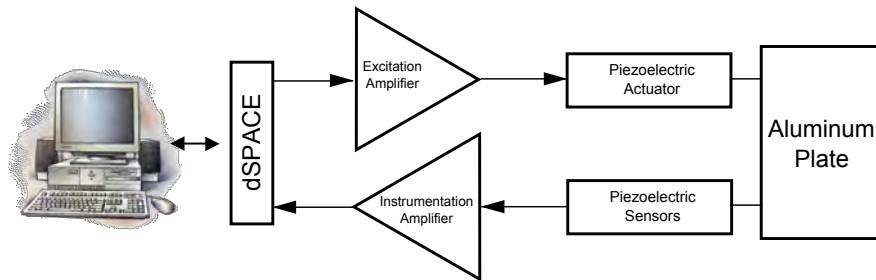


Figure 4. Block diagram of the experiment setup

Damage will significantly alter the measured dynamic response, due to changes in stiffness, mass or energy dissipation (Sohn *et al.*, 2004). In order to test the performance of the SHM proposed approach, several calibrated damage are introduced at different localization on the plate. Thus, masses of 2.5g, 8.5g and 20g are added at specific places to evaluate the efficiency of the monitoring algorithm to detect, locate and diagnosis the damage. With these masses, it was initially created four configurations caused by interaction between plate and masses, as follows:

1. No mass on the plate (healthy plate);
2. Mass of 2.5g on position $(-210, -50)$ (damage 1);
3. Mass of 8.5g on position $(-210, -50)$ (damage 2);
4. Mass of 20g on position $(-210, -50)$ (damage 3).

Figure 5 shows masses position on the aluminum plate for configurations 2, 3 and 4. For each configuration, eight AR models are identified. In configuration 1, the eight healthy models are considered as reference. Thus, using the subspace metric, each reference model can be compared with their respective model for the different configurations. For example, the healthy s_1 model is compared with s_1 model of configuration 2.

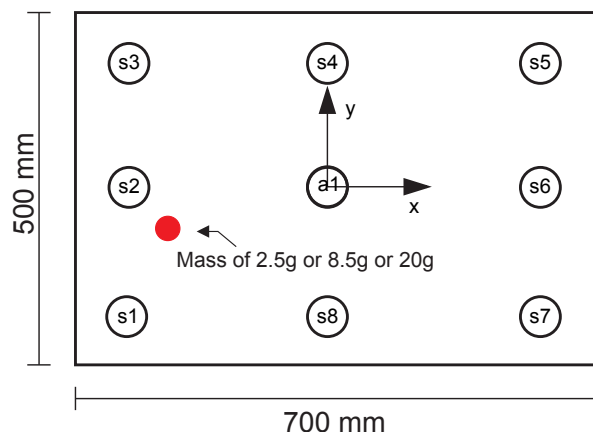


Figure 5. Masses position for configurations 2 to 4

Figure 6 presents the differences between reference models and models of configurations 2, 3 and 4, using the subspace metric. Note that all masses produce differences between models, but this difference increases with the mass weight and with proximity to the sensor. Thus, subspace metric is able to detect damage and quantify its severity. Also, in the region between sensors s_1 and s_2 , where the masses were placed, the models had the greatest difference. Thereby, subspace metric can be used to locate damage.

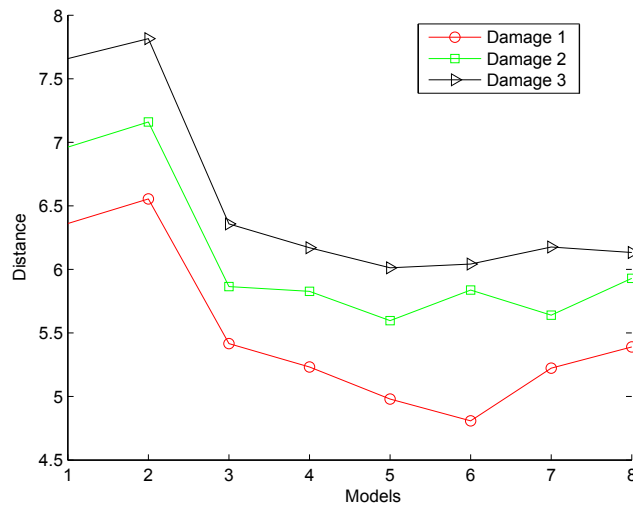


Figure 6. Distance between reference and damaged plate models for configurations 2, 3 and 4

To prove that the technique is also effective to locate damage, two new configurations are tested (Fig. 7):

5. Mass of 20g on position $(-210, -50)$ and mass of 2.5g on the position $(70, 150)$ (damage 4).
6. Mass of 20g on position $(-210, -50)$ and mass of 8.5g on the position $(70, 150)$ (damage 5).

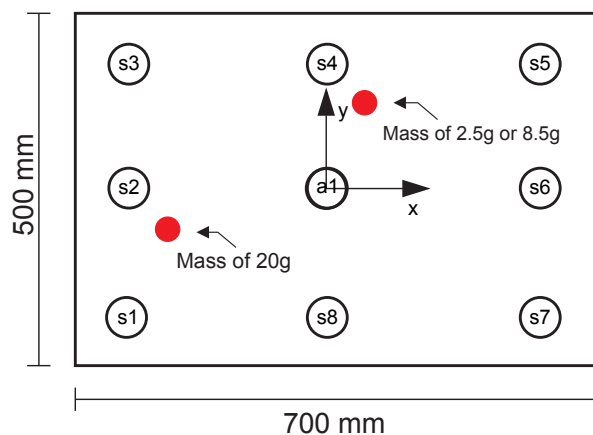


Figure 7. Masses position for configurations 5 and 6

The distance between the reference models for configurations 5 and 6 is presented in Fig. 8. Also in this case, the difference increases with the mass weight and with proximity to the sensor. It can be seen that there are two regions where the difference is greater: between sensors s_1 and s_2 , and between sensors s_4 and s_5 . These regions coincide with positions of the masses. Thus, subspace metric proves to be an efficient method for damage detection, analysis of damage severity and as damage localization indicator.

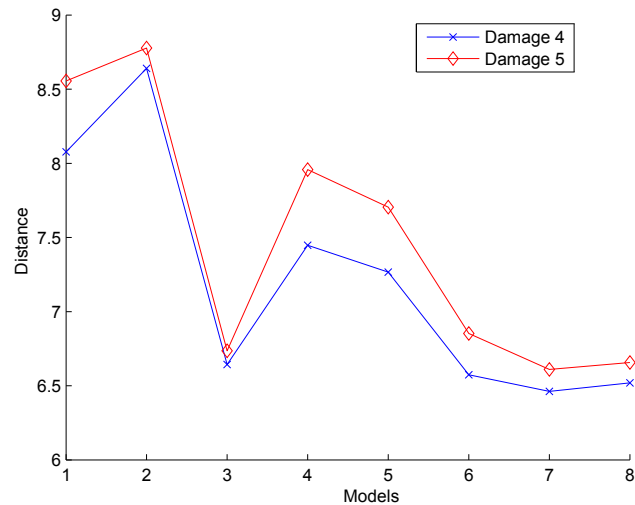


Figure 8. Distance between reference and damaged plate models for configurations 5 and 6

4. CONCLUSION

Experimental results based on subspace metric and subspace identification for SHM purpose were reported. A rectangular aluminum plate was used for the experiment and three masses of $2.5g$, $8.5g$ and $20g$ were placed on the plate, in specific places, to simulate damages. Using eight piezoelectric sensors and one piezoelectric actuator, eight SISO systems were identified using subspace algorithm, one for each sensor/actuator pair. The eight systems of the plate without damage were considered as reference models and, for each damage simulation, eight other systems were identified. Subspace metric between healthy and damage configurations have been calculated and residues were analyzed for SHM purpose.

The subspace metric proved to be efficient in identifying damages, their locations and severity in these real applications. However, some questions remain to be investigated, such as using it on complicated structures, which are going to be object of future developments.

5. ACKNOWLEDGEMENTS

The authors Helói F. G. Genari and Eurípedes G. O. Nóbrega are supported through grants from CAPES and CNPq.

6. REFERENCES

- Bodeux, J.B. and Golival, J.C., 2003. "Modal identification and damage detection using the data-driven stochastic subspace and ARMAV methods". *Mechanical Systems & Signal Processing*, Vol. 17, No. 1, pp. 83–89.
- Carden, E.P. and Fanning, P., 2004. "Vibration based condition monitoring: A review". *Structural Health Monitoring*, Vol. 3, No. 4, pp. 355–377.
- De Cock, K. and De Moor, B., 2002. "Subspace angles between ARMA models". *Systems and Control Letters*, Vol. 46, No. 4, pp. 265–270.
- Desai, U.B. and Pal, D., 1982. "A realization approach to stochastic model reduction and balanced stochastic realizations". In *21st Decision and Control Conference*. Orlando, FL, pp. 1106–1112.
- Fan, W. and Qiao, P., 2010. "Vibration-based damage identification methods: A review and comparative study". *Structural Health Monitoring*.
- Fassois, S.D. and Sakellariou, J.S., 2007. "Time series methods for fault detection and identification in vibrating structures". *Phil. Trans. R. Soc. A*, Vol. 365, pp. 411–448.
- Genari, H.F.G. and Nobrega, E.G.O., 2012. "A damage detection technique based on ARMA models distance estimation". In *Proceedings of the 1st International Symposium on Uncertainty Quantification and Stochastic Modeling - Uncertainties 2012*. São Sebastião, Brazil.
- Humar, J., Bagchi, A. and Xu, H., 2006. "Performance of vibration-based techniques for the identification of structural damage". *Structural Health Monitoring*, Vol. 5, No. 3, pp. 215–241.
- Inocente-Junior, N.R., Nóbrega, E.G.O. and Mechbal, N., 2009. "Real-time structural damage detection using parity residue analysis". In *Proceedings of the 20th International Congress of Mechanical Engineering - COBEM2009*. Gramado, Brazil.
- Katayama, T., 2005. *Subspace Methods for System Identification*. Springer-Verlag.

22nd International Congress of Mechanical Engineering (COBEM 2013)
November 3-7, 2013, Ribeirão Preto, SP, Brazil

- Lu, Y. and Gao, F., 2005. "A novel time-domain autoregressive model for structural damage diagnosis". *Journal of Sound and Vibration*, Vol. 283, pp. 1031–1049.
- Martin, R.J., 2000. "A metric for ARMA process". *IEEE Transactions on Signal Processing*, Vol. 48, No. 4, pp. 1164–1170.
- Nair, K.K., Kiremidjian, A.S. and Law, K.H., 2006. "Time series-based damage detection and localization algorithm with application to the asce benchmark structure". *Journal of Sound and Vibration*, Vol. 4, No. 1-2, pp. 349–368.
- Overschee, P.V. and Moor, B.D., 1996. *Subspace Identification for Linear Systems*. Kluwer Academic Pub.
- Ren, W.X., Lin, Y.Q. and Fang, S.E., 2011. "Structural damage detection based on stochastic subspace identification and statistical pattern recognition: I. theory". *Structural Health Monitoring*.
- Saeed, K., Mechbal, N., Coffignal, G. and Vergé, M., 2009a. "Artificial neural network based structural damage diagnosis using non-parametric subspace residual". In *7th International Workshop on Structural Health Monitoring - IWSHM*. Stanford, USA.
- Saeed, K., Mechbal, N., Coffignal, G. and Vergé, M., 2009b. "Structural damage diagnosis using subspace based residual and artificial neural networks". In *7th IFAC Symposium on Fault Detection, Supervision and Safety of Technical Processes - SafeProcess2009*. Barcelona, Spain.
- Sohn, H., Farrar, C.R., Hemez, F.M., Shunk, D.D., Stinemates, D.W., Nadler, B.R. and Czarnecki, J.J., 2004. "A review of structural health monitoring literature: 1996-2001". Technical reports, Los Alamos National Laboratory.
- Worden, K. and Dulieu-Barton, J.M., 2004. "An overview of intelligent fault detection in systems and structures". *Structural Health Monitoring*, Vol. 3, No. 1, pp. 85–98.
- Zhen, W. and Zhigao, Z., 2010. "Damage detection of offshore platform structures using time domain response data". In *Proceedings of the 2010 International Conference on Intelligent Computation Technology and Automation - ICICTA*. IEEE, Changsha, China, pp. 1079–1084.
- Zheng, H. and Mita, A., 2008. "Damage indicator defined as the distance between ARMA models for structural health monitoring". *Struct. Control Health Monit.*, Vol. 15, pp. 992–1005.
- Zheng, H. and Mita, A., 2007. "Two-stage damage diagnosis based on the distance between ARMA models and pre-whitening filters". *Smart Materials and Structures*, Vol. 16, pp. 1829–1836.

7. RESPONSIBILITY NOTICE

The authors are the only responsible for the printed material included in this paper.